Mitteilungen des naturwissenschaftlichen Vereines für Steiermark	Bd. 140	S. 45–67	Graz 2010

Eclogitized Gabbros from Gressenberg, Koralpe, Austria: Transformation phenomena and their interpretation

Von Alexander Proyer[1] & Walter Postl[2]
Mit 6 Abbildungen und 2 Tabellen

Angenommen am 27. Oktober 2010

Zusammenfassung: **Eklogitisierte Metagabbros von Gressenberg, Koralpe: Umwandlungsphänomene und deren Interpretation.** – Die von der altalpidischen (eo-alpinen) Metamorphose überprägten Metagabbros von Gressenberg zeigen als weltweite Rarität direkt die Reaktionsfront im Übergang von Gabbro zu Eklogit. Der magmatische Plagioklas zerfällt im Kern zu Zoisit und einem Na-reicheren Plagioklas und randlich zu einem extrem feinkörnigen Filz von Klinopyroxen und Kyanit. Der magmatische Orthopyroxen entwickelt eine Klinopyroxen-Spinell-Korona, die sich bei weiterer Überprägung zu einer Granat-Klinopyroxen-Korona weiterentwickelt, in der der Granat mengenmäßig immer dominanter und der Klinopyroxen immer Na-reicher (Hochdruck-Omphazit) wird. Innerhalb der Korona und an deren Rändern bilden sich weitere metastabile Al-reiche Minerale, Korund und Kyanit, die in der Folge von Granat aufgezehrt werden. Die Bildungsreaktionen der einzelnen Zonen und Minerale werden mit Gleichungen für offene chemische Systeme qualitativ beschrieben, wobei die Kriterien Ladungsausgleich und Volumenskonstanz berücksichtigt werden. Vergleiche mit anderen Vorkommen koronitischer Metagabbros zeigen, dass die an sich einfach erscheinende Vorgabe von chemischen Potenzialgradienten zwischen Plagioklas und den mafischen Phasen Orthopyroxen und Olivin die große texturelle und mineralogische Vielfalt nicht erklären kann, und weitere Einflussgrößen berücksichtigt werden müssen.

Summary: Metagabbros from Gressenberg have undergone an eo-Alpine eclogite-facies overprint and are unique because the immediate reaction front at the transition gabbro-eclogite can be seen. Magmatic plagioclase decomposes to zoisite and a more sodium-rich plagioclase in the core, and to a very fine-grained intergrowth of clinopyroxene and kyanite at the rim. Magmatic orthopyroxene first develops a clinopyroxene-spinel corona which is replaced subsequently by a garnet-clinopyroxene corona in which garnet becomes modally dominant and clinopyroxene more jadeitic (high-pressure omphacite) with increasing degree of overprint. Within the corona and at its margins metastable Al-rich minerals develop (corundum and kyanite), which are subsequently replaced by garnet. The reactions forming single zones or minerals are formulated with open-system equations which take into account both charge and volume balance. A comparison with other occurrences of coronitic metagabbros worldwide shows that the simple boundary conditions of chemical potential gradients between plagioclase and mafic phases (olivine and orthopyroxene) are insufficient to explain the textural and mineralogical variations and other factors need to be taken into account as well.

1. Introduction

The Koralpe in southeastern Austria is famous for its occurrences of eo-Alpine (ca. 90 Ma) eclogites (Thöni & Miller 1996, Gregurek & al. 1997, Bruand & al. 2010) which – contrary to their counterparts from the nearby Saualpe – are mostly not coarse-grained but often preserve the gabbroic protolith and develop fine grained decomposition textures which reflect the kinetics of the transformation into eclogite by limited infiltration of fluid (Thöni & Jagoutz 1993). There are a number of occurrences worldwide

---

[1] Alexander Proyer, Institut für Erdwissenschaften, Karl-Franzens-Universität Graz, Universitätsplatz 2/II, A-8010 Graz, Austria, E-Mail: alexander.proyer@uni-graz.at

[2] Walter Postl, c/o Abteilung für Mineralogie, Studienzentrum Naturkunde, Universalmuseum Joanneum, Weinzöttlstraße 16, A-8045 Graz, Österreich, E-Mail: walter.postl@gmx.at

where similar textural features of a disequilibrium transformation from dry gabbro into a hydrated eclogitic assemblage have been described, as will be shown in the discussion section. However, the sample presented in this work is particularly attractive and unique because the immediate reaction/hydration front is preserved. Rocks of this character were investigated already by Weber (1941) and Heritsch (1973), and more recently by Kuntze & al. (2007), but no detailed results have been published by the latter authors. The occurrence itself is a large, about 12 km^2 sized field of blocks of mainly eclogite and metagabbro in Gressenberg, southwest of Deutschlandsberg (Winkler 1966). A group of blocks showing this very rare type of small scale proximity and transition between the magmatic protolith and its metamorphic equivalent were found in the year 2000 by one of the authors (W. P.) about 450 m west of the farm Weberbauer (15°05'13"E, 46°45'00"N). The largest and most impressive of those blocks has subsequently been sawed and polished and is now on display at the Geopark Glashütten (Fig. 1a) in the district of Gressenberg (Postl 2009). The thin sections used in this work come from a 100–200 kg block from the same locality, and were cut adjacent to each other in a sequence across the visible gabbro-eclogite reaction front (Fig. 1b).

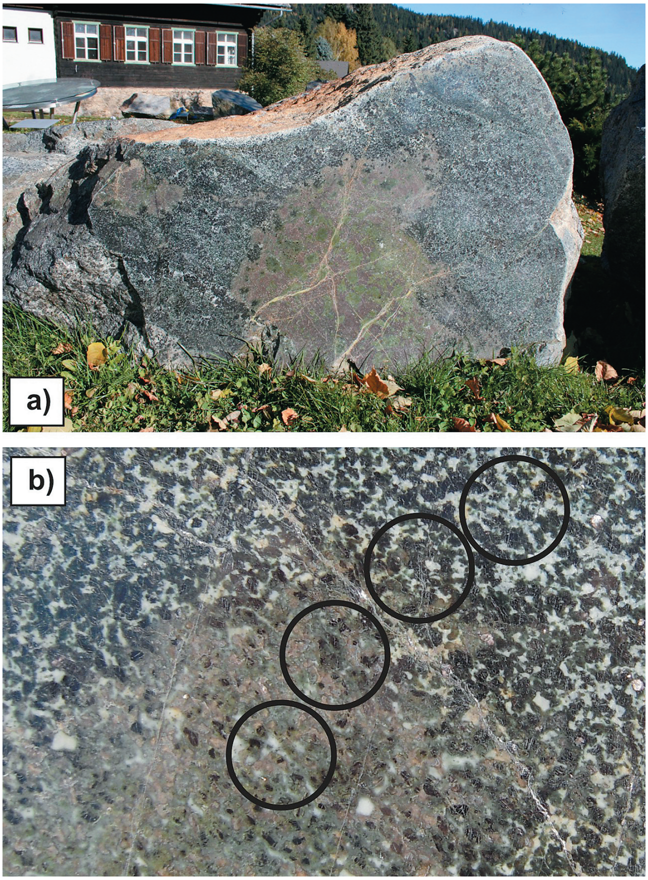

Fig. 1: a) Large boulder from the Gressenberg area, now on display at Geopark Glashütten. It shows the impressive transition from gabbro to eclogite along a fluid infiltration front; b) polished hand specimen of a similar sample with infiltration front; circles are 20 mm in diameter and indicate locations of thin sections from top right (1WP) to bottom left (4WP).

The present investigation was performed with a scanning electron microscope (SEM) equipped with microanalytical facilities (EDX) and allowed a much better spatial resolution and analytical precision compared to previous works. It revealed a surprising variety of metastable, intermediate reaction products, which are interpreted to be the expression of very small "volumes of equilibration" or "effective bulk compositions", ever decreasing with distance from the main pathways of incoming fluid. Going along with this enhancement of reaction kinetics by fluid molecules is a change in mineral assemblage (types of minerals which co-exist), an increase in grain size, a flattening in zoning patterns and a change in apparent metamorphic grade: neither garnet nor omphacite, the minerals defining eclogite, are present as early replacement products of metagabbro. In the more equilibrated samples they are – only millimetres to centimetres away. In this contribution, the textures are described in detail, together with information on mineral compositions, suggested reaction equations and conclusions about the nature of the fluid and the chemical potential gradient evolution with increasing fluid access and time of reaction.

2. Petrography and mineral chemistry

2.1 Protolith

Mineral relics of the gabbro protolith can be found in most sections but are best preserved in thin sections 1WP and 2WP (Fig. 1b). The gabbro consisted of large, chemically homogenous crystals of plagioclase, orthopyroxene (bronzite), and clinopyroxene (augite) as well as the rare accessory pyrrhotite. Neither olivine nor quartz has been found in any of the sections. Magmatic clinopyroxene displays oriented inclusions (precipitates) of ilmenite. The compositions of magmatic minerals are given in Table 1. Plagioclase has $X_{an} = 0.75$ and both pyroxenes are slightly aluminous.

2.2 Section 1WP

Plagioclase has developed a concentric textural pattern with preserved original plagioclase in the core, crosscut and replaced by newly grown laths of zoisite which are accompanied by more albite-rich plagioclase (Fig. 2a, c). The outer zone is composed of a very fine-grained intergrowth of clinopyroxene and needles of kyanite (Fig. 2b). In some plagioclase sites, there is an intermediate zone, where zoisite, albitic plagioclase, clinopyroxene and kyanite occur next to each other. (Mineral intergrowth is usually so fine-grained that the analyses given in Table 1 for this textural site may to some extent represent phase-mixes due to "beam overlap", even though the spots for analysis were carefully chosen.) In some cases the original plagioclase-plagioclase grain boundaries are now marked by corundum (Fig. 2a, b).

Orthopyroxene developed coronas of clinopyroxene, which is constant in composition across the corona and includes a number of other, usually very fine grained Al-rich phases: spinel and subordinate corundum and kyanite. Spinel appears as droplets or symplectitic intergrowths with clinopyyroxene (Fig. 2b, d). Small inclusions of relict orthopyroxene in the corona indicate that the corona grows mainly towards orthopyroxene. Spinel is a binary hercynite-spinel solid solution which varies in composition between 44 and 55 Mol% $MgAl_2O_4$. These differences in X_{Mg} of spinel vary with location in the sample, but are constant across a corona in each site. Corona-corundum is very pure (Fe as the only other cation above detection limit remains below ca. 0.3 wt% Fe_2O_3) and in some cases enclosed by kyanite. The distribution of corundum and kyanite throughout a corona can be quite regular, but seems to be concentrated in some cases along the outer and inner margins of the corona.

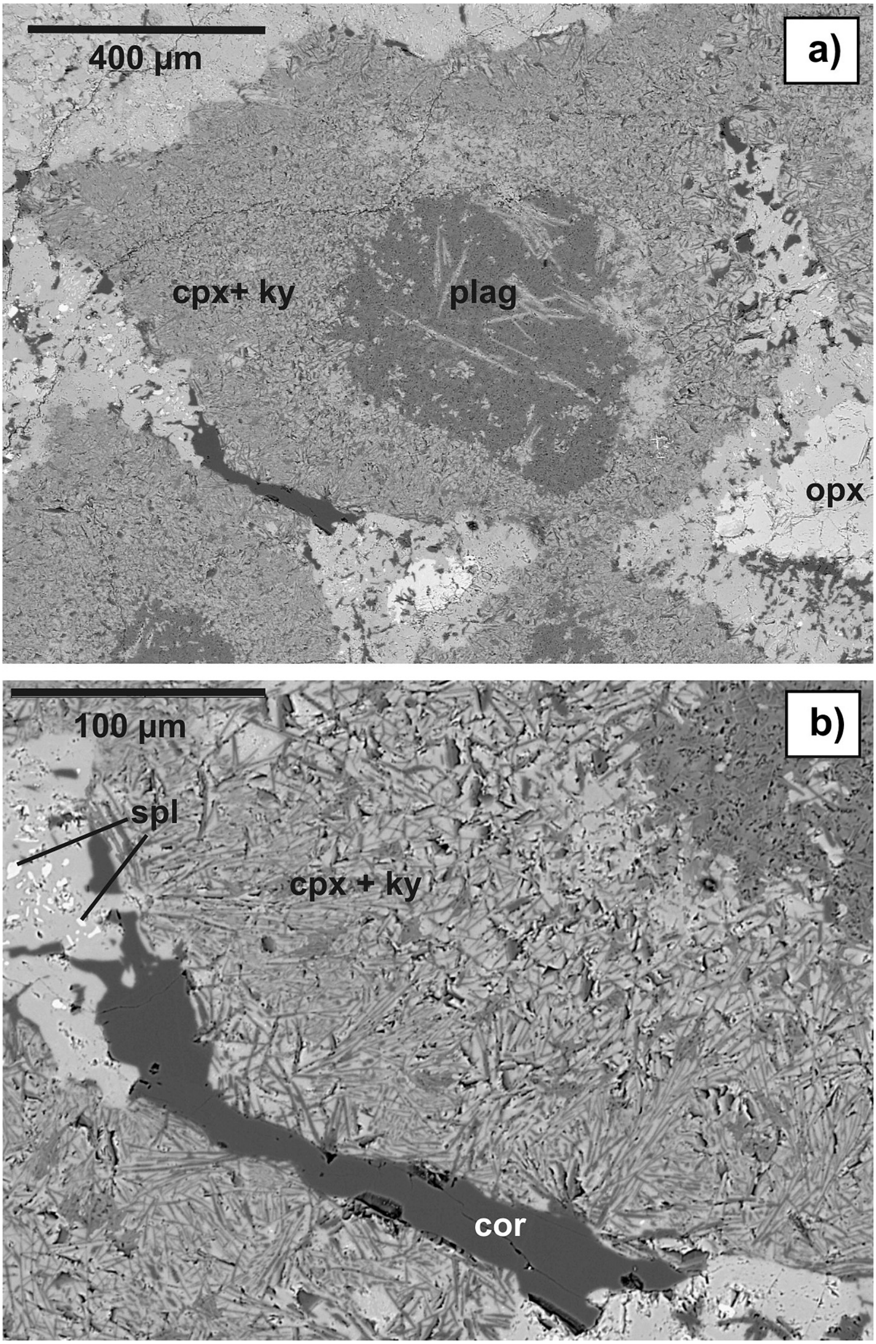

Fig. 2 (1WP): a) Decomposition textures of igneous plagioclase (i-plag) amongst orthopyroxene (opx). Inner zone of zoisite + Na-richer metamorphic plagioclase (m-plag), outer zone of new clinopyroxene (m-cpx) + kyanite + some m-plag; opx with coronae of cpx + spl, with some inclusions of kyanite and corundum; thick lath of corundum at former plag-plag grain boundary; b) Detail of 1a showing fine intergrowth of kyanite-hairs with m-cpx and subordinate m-plag; some kyanite needles also in the cpx-free inner core;

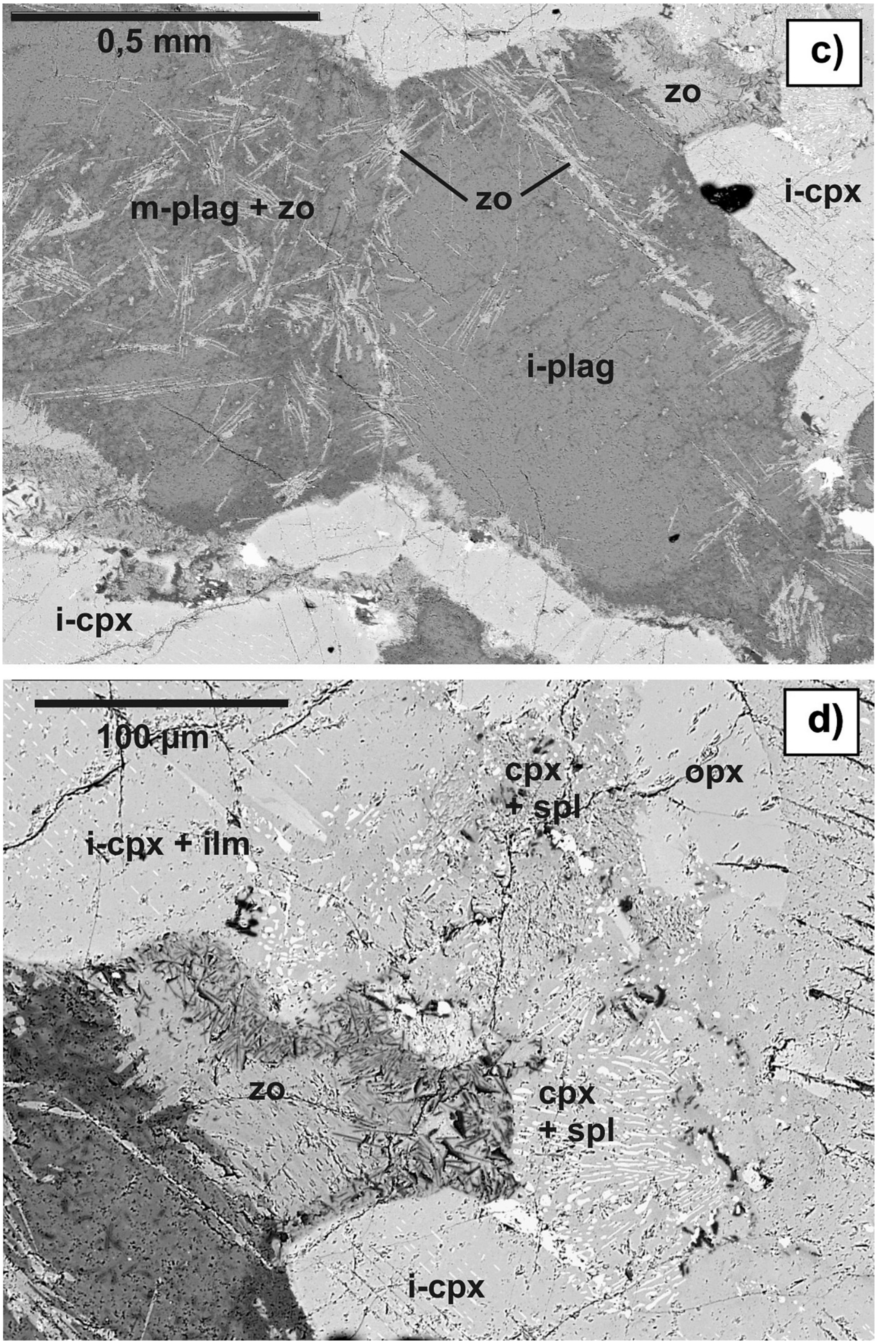

Fig. 2 (1WP) c) i-plag is hardly decayed when enclosed almost entirely by i-cpx: well preserved core and subordinate decomposition into zoisite + new sodic plagioclase; d) detail of grain boundary where opx is involved: thin cpx-ky-corona and spinel-dotted and symplectitic clinopyroxene as reaction products of plag with small opx in cpx; note oriented ilmenite lamellae in i-cpx.

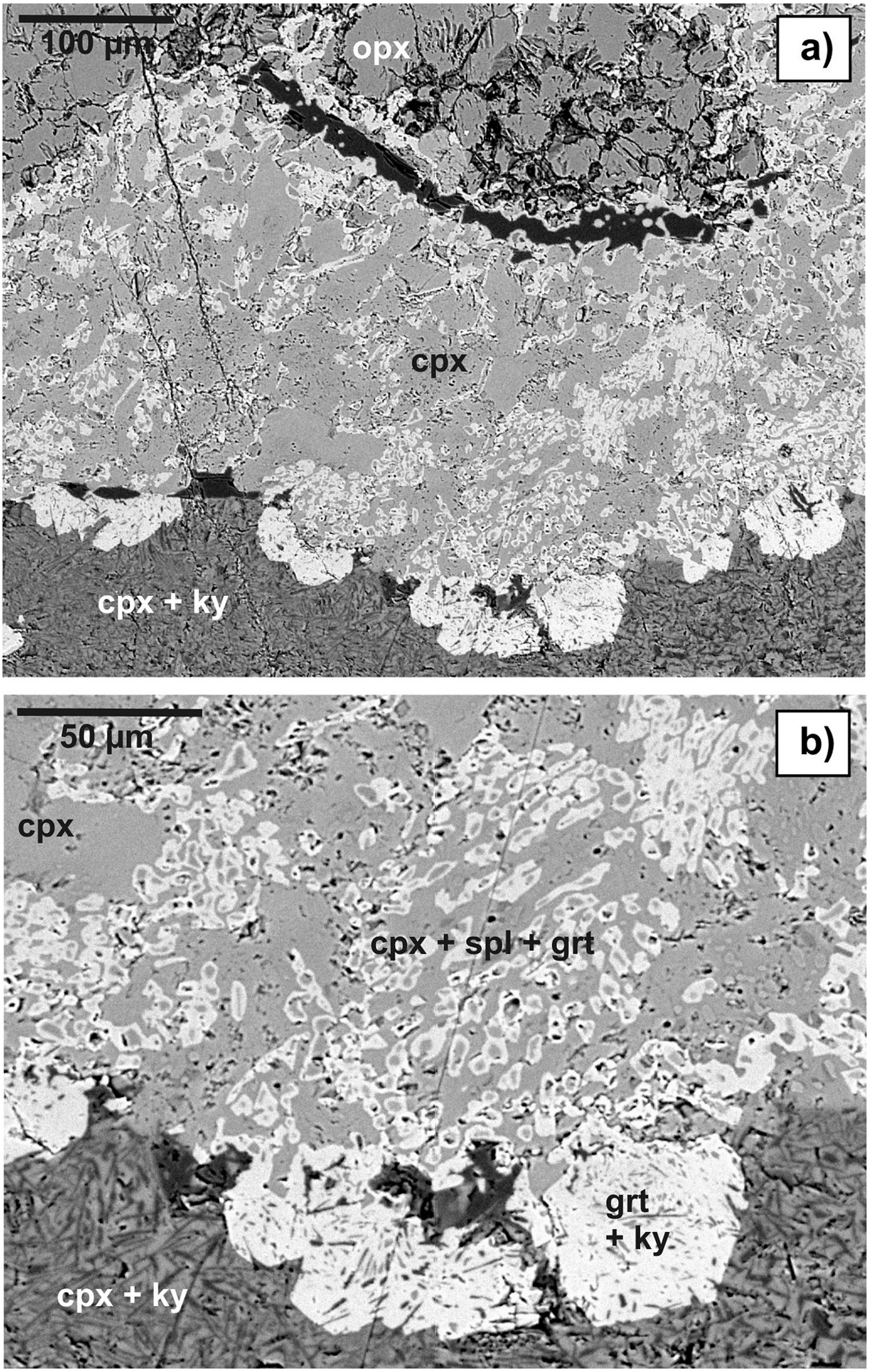

Fig. 3 (1WP): a) more strongly overprinted corona where spinel is replaced by (white) garnet; the Al-rich phases (black) tend to be concentrated at either margin of the corona: corundum at the opx-side, kyanite at the i-plag domain-boundary; b) detail of 3a, showing idiomorphic garnet overgrowing the cpx-ky-domain and preserving some of the kyanite needles as inclusions;

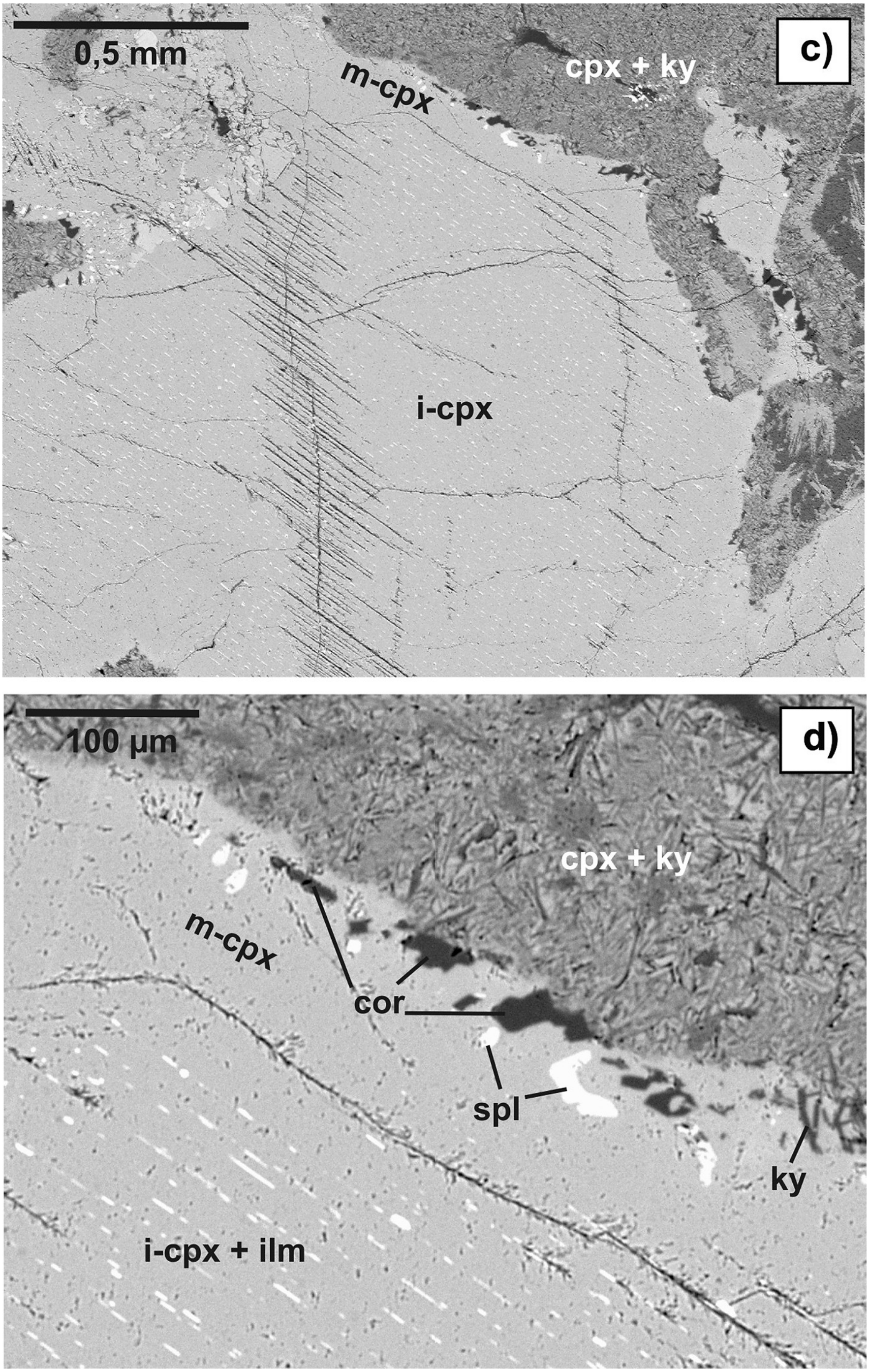

Fig. 3 (1WP): c) i-cpx acquires small growth rims of slightly more sodic m-cpx; d) at some places this rim also contains small crystals of spinel, corundum and kyanite.

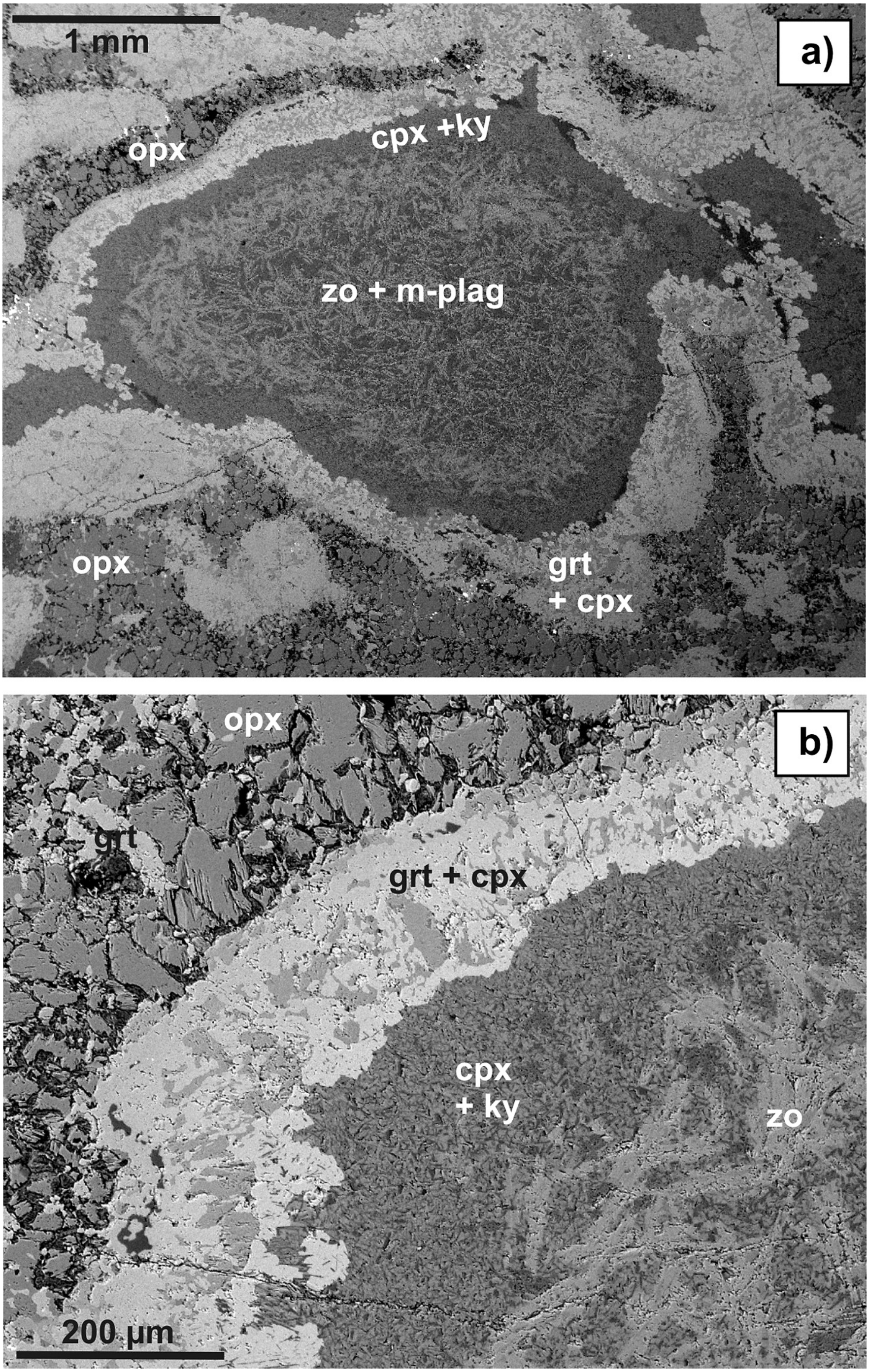

Fig. 4 (2WP): a) advanced stage of recrystallization of former i-plag site with large zoisite + sodic plagioclase ± kyanite core and fully garnetized corona towards i-opx; b) detail of 4a shows coarsened zoisite grain size, garnet predominance in corona over cpx and garnet growth advancing into opx;

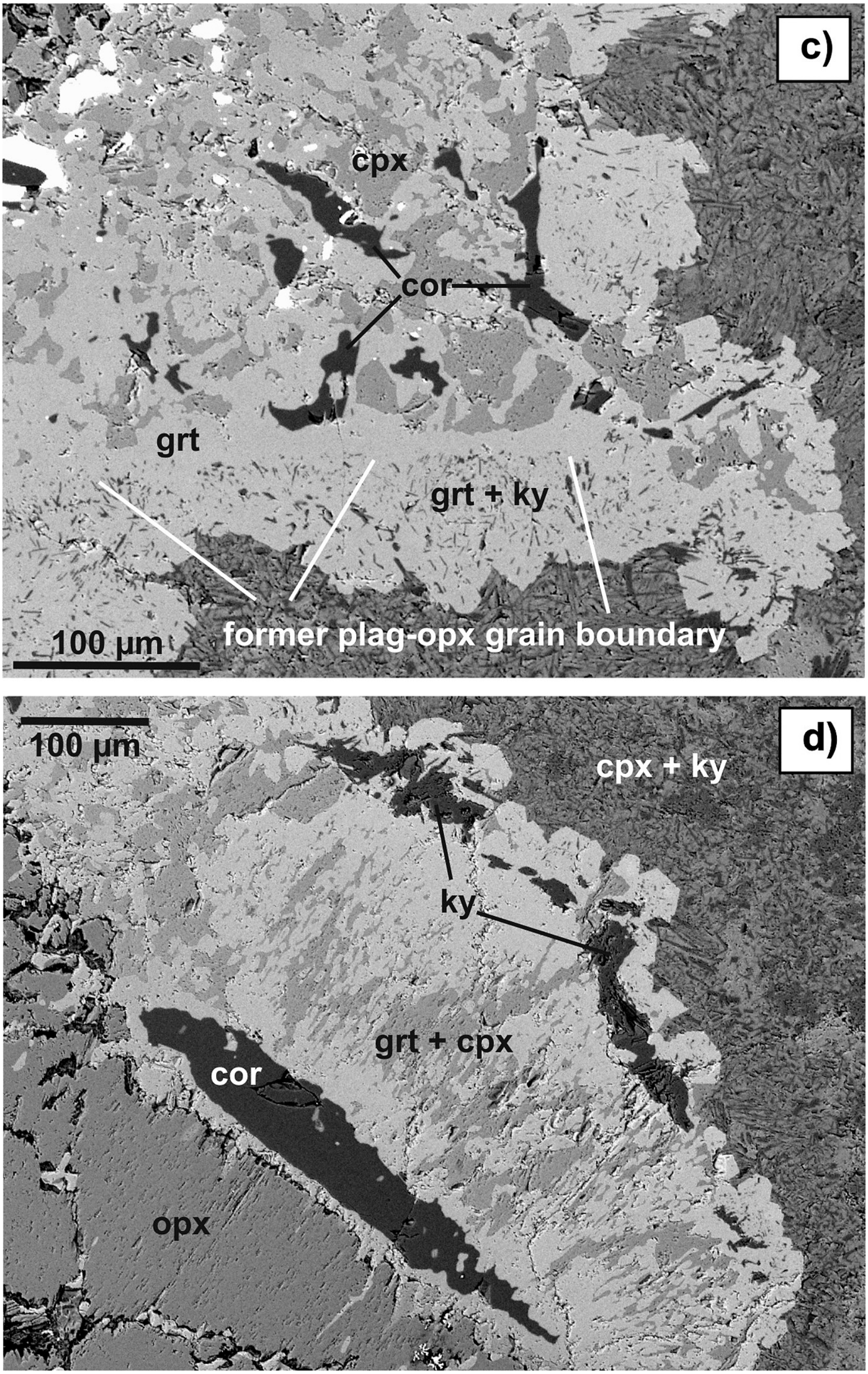

Fig. 4 (2WP): c) detail of a corona with Al-rich phases showing suggested position of igneous plag-opx grain boundary; d) another corona site with two-sided concentration of garnet-enclosed Al-rich phases similar to Fig. 2c.

In some regions of 1WP garnet is observed as a new phase which grows at the corona site: as overgrowths on small droplets of spinel within the corona and as larger crystals with partly idiomorphic faces and including very fine grained needles of kyanite along the corona rim towards the site of former plagioclase, indicating progressive overgrowth of the former plagioclase site (Fig. 3a, b). This garnet is the brightest of all phases in backscattered electron (BSE) contrast. For compositions see Table 1.

Clinopyroxene is least affected by the alteration process. It develops relatively thin growth regions along some of its grain boundaries with virtually identical contrast in BSE images and almost identical chemical composition (see Table 1). This new generation of clinopyroxene can mainly be distinguished by its lack of ilmenite precipitate lamellae, and sometimes by minor inclusions of spinel, corundum or kyanite (Fig. 3c, d).

2.3 Section 2WP

More magmatic plagioclase grains are now entirely decomposed, with slightly coarser intergrowths of zoisite with a more sodic metamorphic plagioclase in the core (X_{an} = 0.25–0.35), a transition zone, where plagioclase (X_{an} = 0.30–0.38) and zoisite are found adjacent to clinopyroxene (X_{jd} = 0.30) and acicular kyanite and a rim zone of clinopyroxene + kyanite (Fig. 4a). Most clinopyroxene in this rim zone has the Na/Ca ratio of the original plagioclase, which translates into an X_{jd} of 0.23–0.26. Tiny relic plagioclase in this region has X_{an} = 0.36–0.39.

The coronae around orthopyroxene are coarser in grain size and turned into a garnet-clinopyroxene intergrowth, with no more spinel and somewhat rarer inclusions of corundum and kyanite in the central parts and tiny kyanite needles in garnet overgrowing the fine grained intergrowth of clinopyroxene + kyanite of the plagioclase site (Fig. 4b–d).

Most coronae are devoid of corundum and kyanite but show concentrations of these phases at their inner and outer margins (Fig. 4d). Garnet is compositionally zoned across the corona, with constant X_{alm} and X_{spe} but a variation in pyrope and grossular content from $pyr_{56}alm_{29}gro_{13}spe_{2}$ on the orthopyroxene side to $pyr_{33}alm_{30}gro_{36}spe_{1}$ on the plagioclase side of the corona. Clinopyroxene becomes more sodic towards the plagioclase side but varies in X_{jd} only between 0.07 and 0.11. Garnet is no longer restricted to the corona, but also grows as tiny droplets within some orthopyroxenen grains. In other cases, the corona around orthopyroxene becomes a double corona, with an inner ring of inclusion-free clinopyroxene.

The metamorphic rims of magmatic clinopyroxene show a marked increase in Na from 0.08 to 0.18 a.p.f.u. accompanied by Al, which goes from 0.12 to 0.20 – mainly at the expense of Mg and Ca, which drop from 0.83 to 0.76 and from 0.91 to 0.82, respectively. Disregarding the ambiguities of Fe^{3+}-determination, this indicates mainly a decrease in diopside and Tschermakite component, and an increase in jadeite component of the clinopyroxene, which is now almost omphacite. Other metamorphic rims with a less pronounced increase in jadeite content (very similar to the corona-cpx around opx) have been observed and measured as well, indicating variable chemical potential conditions in the same type of setting.

2.4 Section 3WP

The central parts of former plagioclase sites are coarser in grain size and consist mainly of zoisite, kyanite, clinopyroxene and some albite-rich plagioclase. The marginal parts are still composed of fine-grained clinopyroxene-kyanite intergrowths.

Tab. 1: Analyses of igneous phases and minerals outside the coronas.
Anlysen von magmatischen und Nicht-Korona-Mineralen.

Mineral	**1WP**			**1WP**	**2WP**	**3WP**	**4WP**	
	igneous phases			**rim on i-cpx**		**opx-site**	**opx-site**	**plag-site**
	cpx	**opx**	**plag**	**cpx**	**cpx**	**amph**	**amph**	**amph**
SiO_2	52.89*	54.03	49.46	52.47	54.60	55.89	49.00	49.53
Al_2O_3	2.53	2.98	31.92	3.96	5.34	4.44	9.62	10.65
Fe_2O_3	0.00	0.00	0.00	0.00	0.00	0.00	0.00	0.00
FeO	6.39	15.29	0.00	4.40	2.77	3.59	5.20	4.06
MgO	16.64	27.38	0.00	14.70	2.56	22.15	17.66	19.13
CaO	18.97	0.34	15.13	22.38	20.63	11.19	11.49	11.75
MnO	0.16	0.19	0.00	0.17	0.00	0.00	0.18	0.00
Na_2O	0.65	0.00	3.06	0.88	2.56	0.92	1.80	1.88
Total	**98.23**	**100.21**	**99.57**	**98.96**	**88.46**	**98.18**	**94.95**	**97.00**

Formula								
Si	1.96*	1.94	2.27	1.93	2.19	7.59	7.00	6.90
Al	0.11	0.13	1.72	0.17	0.25	0.71	1.62	1.75
Fe^{3+}	0.01	0.00	0.00	0.02	0.00	0.20	0.31	0.24
Fe^{2+}	0.19	0.45	0.00	0.11	0.09	0.21	0.31	0.24
Mg	0.92	1.46	0.00	0.81	0.15	4.49	3.76	3.97
Ca	0.76	0.01	0.74	0.88	0.89	1.63	1.76	1.75
Mn	0.01	0.01	0.00	0.01	0.00	0.00	0.02	0.00
Na	0.05	0.00	0.27	0.06	0.20	0.24	0.50	0.51
O	6	6	8	6	6	23	23	23

Mineral	**1WP**			**2WP**				
	i-plag site			**i-plag site, rim**		**i-plag site, inner rim**		
	zo	**plag**	**cpx**	**plag**	**cpx**	**cpx**	**plag**	**zo**
SiO_2	41.67	58.26	45.72	58.38	51.57	54.19	59.85	39.40
Al_2O_3	28.21	28.01	18.13	26.63	13.55	10.49	25.71	32.32
Fe_2O_3	2.84	0.00	0.00	0.00	0.00	0.00	0.00	1.09
FeO	0.00	0.00	5.14	0.00	2.15	2.37	0.00	0.00
MgO	1.08	0.00	7.29	0.00	9.88	10.61	0.00	0.25
CaO	23.44	8.21	18.75	8.51	19.37	17.41	7.05	24.83
MnO	0.00	0.00	0.09	0.00	0.00	0.00	0.00	0.00
Na_2O	0.37	6.57	2.81	6.35	3.32	4.34	7.30	0.03
Total	**97.61**	**101.05**	**97.96**	**99.87**	**99.84**	**99.41**	**99.91**	**97.92**

Formula								
Si	3.19	2.57	1.70	2.61	1.85	1.94	2.66	3.00
Al	2.54	1.46	0.79	1.40	0.57	0.44	1.35	2.90
Fe^{3+}	0.16	0.00	0.00	0.00	0.00	0.00	0.00	0.06
Fe^{2+}	0.00	0.00	0.16	0.00	0.06	0.07	0.00	0.00
Mg	0.12	0.00	0.40	0.00	0.53	0.57	0.00	0.03
Ca	1.92	0.39	0.75	0.41	0.74	0.67	0.34	2.03
Mn	0.00	0.00	0.00	0.00	0.00	0.00	0.00	0.00
Na	0.06	0.56	0.20	0.55	0.23	0.30	0.63	0.00
O	12.5	8	6	8	6	6	8	12.5

* numbers are weight percent (top) or formula units (bottom) respectively

Tab. 2: Selected analyses of corona minerals.
Ausgewählte Analysen von Korona-Mineralen.

Mineral	**1WP**			**2WP**	**4WP**		
	early corona			**corona-cpx**			
	spl	**spl**	**cpx**	**opx side**	**plag side**	**opx side**	**plag side**
SiO_2	0.00	0.00	52.59	52.71	53.67	54.52	54.25
Al_2O_3	63.78*	65.12	4.58	4.14	3.77	4.43	6.81
Fe_2O_3	0.00	0.00	0.00	0.00	0.00	0.00	0.00
FeO	25.56	22.00	4.24	3.03	2.47	2.41	2.40
MgO	11.19	14.26	14.67	15.47	15.38	14.71	13.55
CaO	0.22	0.20	22.00	23.63	23.31	21.03	19.56
MnO	0.17	0.16	0.00	0.00	0.00	0.00	0.00
Na_2O	0.00	0.00	1.24	1.01	1.54	2.26	3.05
Total	**100.92**	**101.74**	**99.32**	**99.99**	**100.14**	**99.36**	**99.62**

Formula							
Si	0.00	0.00	1.92	1.91	1.93	1.97	1.95
Al	1.99*	1.97	0.20	0.18	0.16	0.19	0.29
Fe^{3+}	0.02	0.03	0.04	0.08	0.07	0.03	0.03
Fe^{2+}	0.55	0.45	0.09	0.02	0.00	0.05	0.05
Mg	0.44	0.55	0.80	0.84	0.83	0.79	0.73
Ca	0.01	0.01	0.86	0.92	0.90	0.82	0.75
Mn	0.00	0.00	0.00	0.00	0.00	0.00	0.00
Na	0.00	0.00	0.09	0.07	0.11	0.16	0.21
O	3	3	6	6	6	6	6

Mineral	**corona garnet**						
	1WP		**2WP**		**3WP**		**4WP**
	opx side	**plag side**	**opx side**	**plag side**	**opx side**	**plag side**	**homog.**
SiO_2	40.12	39.53	41.45	39.93	41.38	40.91	40.50
Al_2O_3	22.50	22.09	22.93	22.04	23.64	23.41	22.20
Fe_2O_3	0.00	0.00	0.00	0.00	0.00	0.00	0.00
FeO	18.50	18.86	15.08	15.18	17.92	17.76	16.00
MgO	11.67	7.68	15.64	8.94	13.15	10.86	12.87
CaO	6.74	11.15	5.27	13.41	6.22	9.32	8.44
MnO	0.41	0.05	0.34	0.23	0.43	0.43	0.36
Na_2O	0.00	0.00	0.00	0.00	0.00	0.00	0.00
Total	**99.94**	**99.36**	**100.71**	**99.73**	**102.74**	**102.69**	**100.37**

Formula							
Si	3.00	3.02	3.01	3.00	2.99	2.98	2.98
Al	1.98	1.99	1.96	1.95	2.01	2.01	1.93
Fe^{3+}	0.02	0.00	0.03	0.05	0.02	0.04	0.10
Fe^{2+}	1.13	1.20	0.89	0.90	1.06	1.05	0.88
Mg	1.30	0.87	1.69	1.00	1.42	1.18	1.41
Ca	0.54	0.91	0.41	1.08	0.48	0.73	0.67
Mn	0.03	0.00	0.02	0.02	0.03	0.03	0.02
Na	0.00	0.00	0.00	0.00	0.00	0.00	0.00
O	12	12	12	12	12	12	12

* numbers are weight percent (top) or formula units (bottom) respectively

The coronae around orthopyroxene show a very strong modal predominance of garnet over clinopyroxene (Fig. 5a, b). This garnet is relatively homogenous in composition, only the innermost parts are a bit higher in Mg and lower in Ca (Tab. 1); Fe is constant throughout. That which appears as an orthopyroxene core at first sight turns out to be amphibole – more precisely a slightly sodic tremolite. Orthopyroxene can still be found as small relics within these large tremolite pseudomorphs. The inner corona of clinopyroxene can be very pronounced or almost entirely missing (Fig. 5a).

At this degree of overprint the grain boundaries between former plagioclase and clinopyroxene have become reactive: garnet is advancing against igneous clinopyroxene, which still shows a marked degree of stability. This garnet grows in a discontinuous, non-coronitic manner. It contains tiny rutile crystals and is very often filled with small acicular kyanite and, in places, with small amounts of quartz that also appears along garnet grain boundaries (Fig. 5c, d).

2.5 Section 4WP

The inner cores of former plagioclase sites develop into relatively coarse-grained intergrowths of zoisite, kyanite and quartz (Fig. 6a, b). The outer parts show a grain coarsening of both clinopyroxene and kyanite, with some interstitial amphibole (Mg-hornblende, Fig. 6c). Amphibole of tremolite to magnesio-hornblende composition often has completely replaced orthopyroxene in the centres of coronae (Fig. 6d). Corona garnet is almost homogenous in composition (Tab. 1), only the corona-cpx is slightly zoned where it still crosscuts the entire corona diameter.

2.6 The textural and compositional evolution of coronas

The first corona is characterised by a very fine-grained to symplectitic intergrowth of clinopyroxene with spinel. The cpx is homogenous in composition across the corona, spinel composition varies in a rather irregular manner. In a second stage, garnet starts to replace the fine droplets of spinel from the rims across the entire corona. Garnet composition indicates a chemical potential gradient in Mg and Ca across the corona, whereas the almandine content is constant throughout.

Corona-clinopyroxene becomes more sodic during continued outward growth (towards former plagioclase sites). After that there is an increasing modal predominance of garnet in the corona, compositional gradients within corona garnet and clinopyroxene are smoothing out.

2.7 The textural and compositional evolution of the former igneous plagioclase site

The most rimward domain is characterized by an apparently instant decay into a fine-grained intergrowth of kyanite and clinopyroxene, which is only recrystallized significantly to coarser grain size in sample 4WP. The interior domain of zoisite + sodic plagioclase is a bit more coarse grained from the beginning and shows a much more pronounced degree of grain coarsening (compared to the outer domain). Both clinopyroxene and kyanite advance towards the central parts with continued degree of overprinting. Clinopyroxene and sodic plagioclase appear to be more sodic towards the core of the plagioclase site, but measurements are not always consistent. In the last stage observed, fine grained kyanite + quartz intergrowths develop in the central parts, but sodic plagioclase is still present, so the final stage of transformation into eclogite has not occurred in this part of the rock. Even the most strongly overprinted samples are still far from chemical and textural equilibration on a cm-scale.

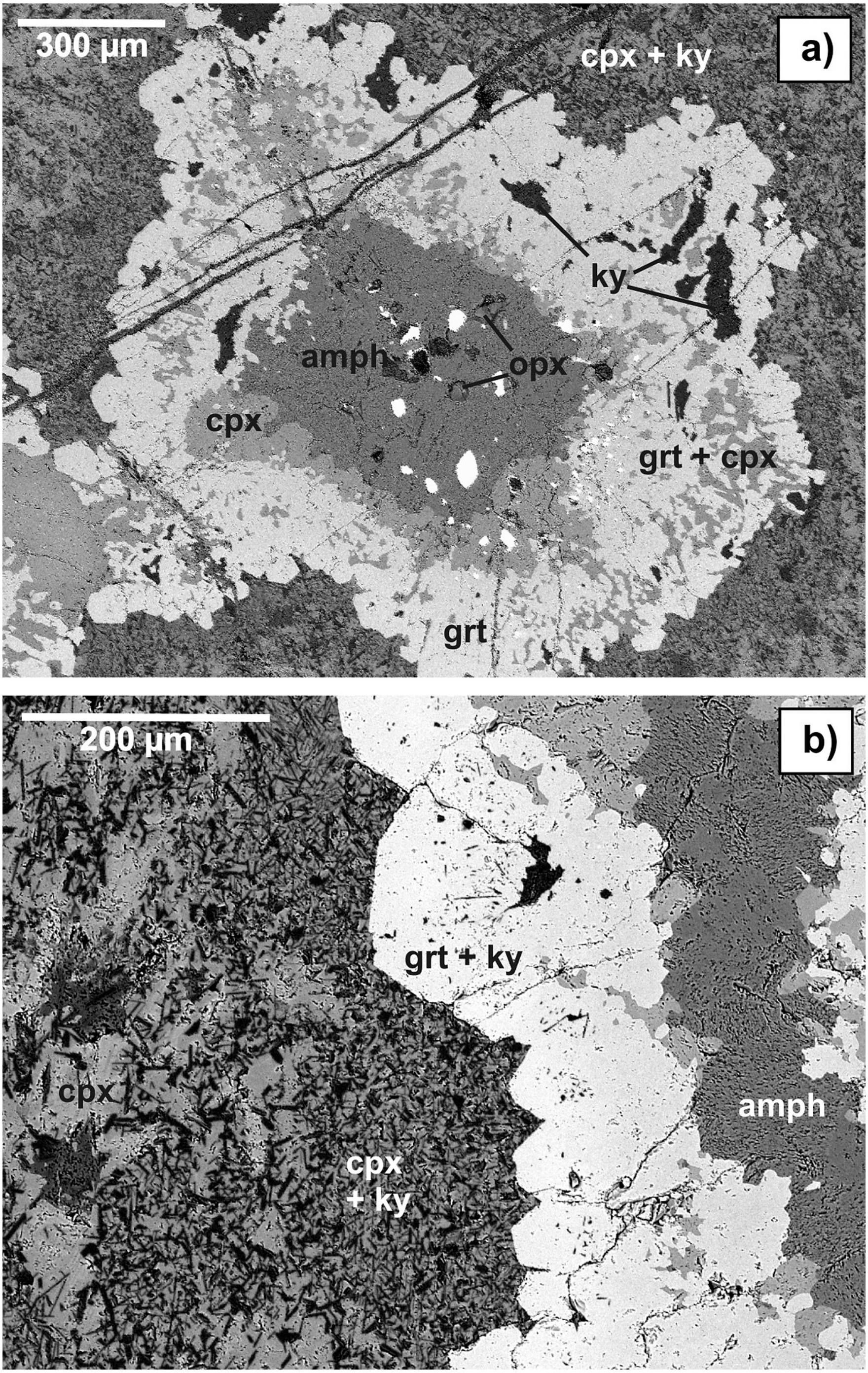

Fig. 5 (3WP): a) coarsened garnet corona with kyanite (dark) and cpx, the latter partly developing into an inner corona. The dark core is mainly amphibole (tremolite), with some tiny relics of opx; the bright grains are Fe-sulfides; b) Corona-detail: note that cpx and kyanite coarsen towards the center of the i-plag domain;

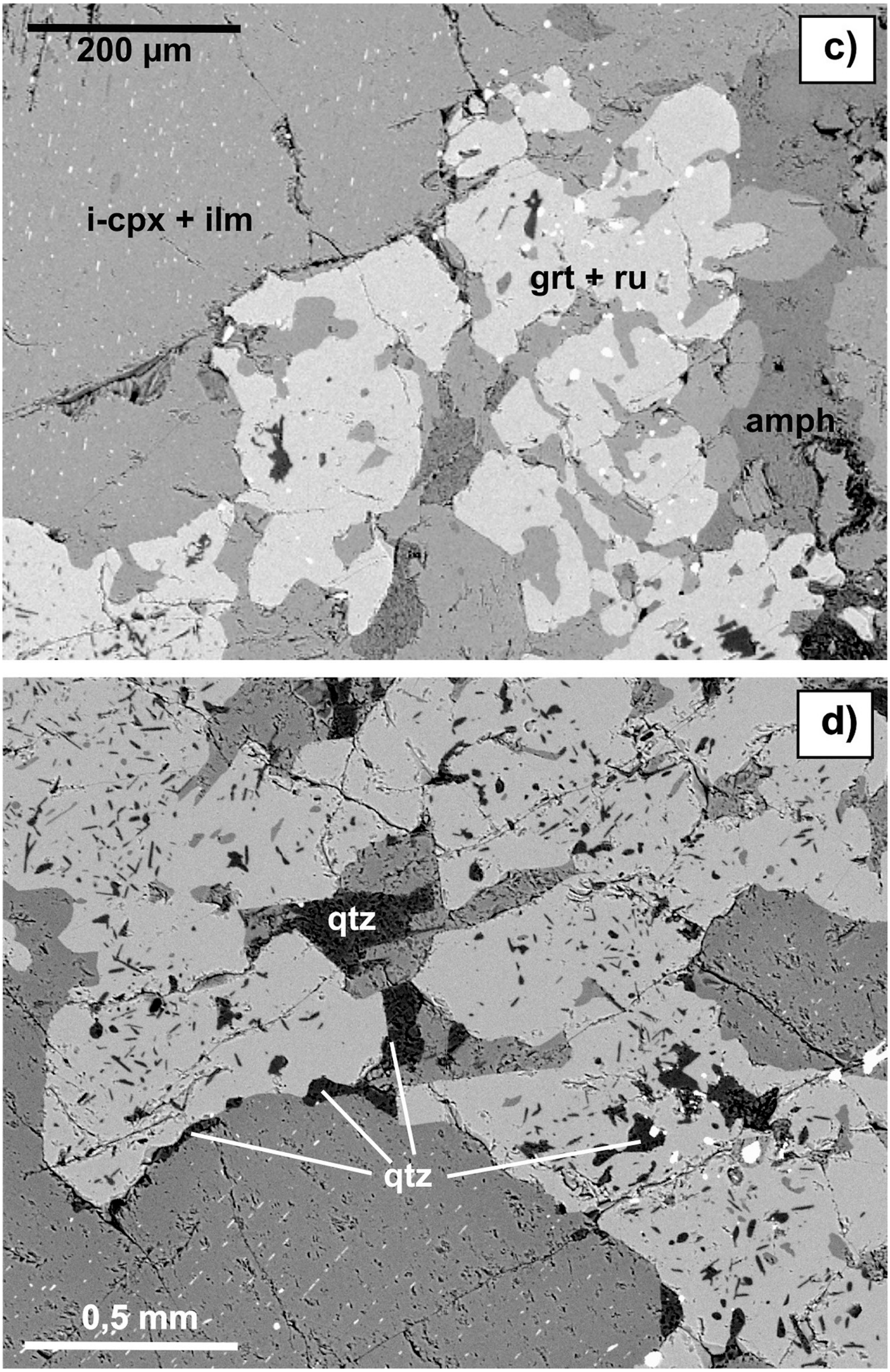

Fig. 5 (3WP): c) garnet growing towards and partly resorbing i-cpx; the white spots are ilmenite in cpx and rutile in garnet; d) garnet (light grey) grown from fingers of former igneous plagioclase in clinopyroxene (medium grey): such garnet not only contains a lot of kyanite (dark) but also the first free quartz observed in these samples.

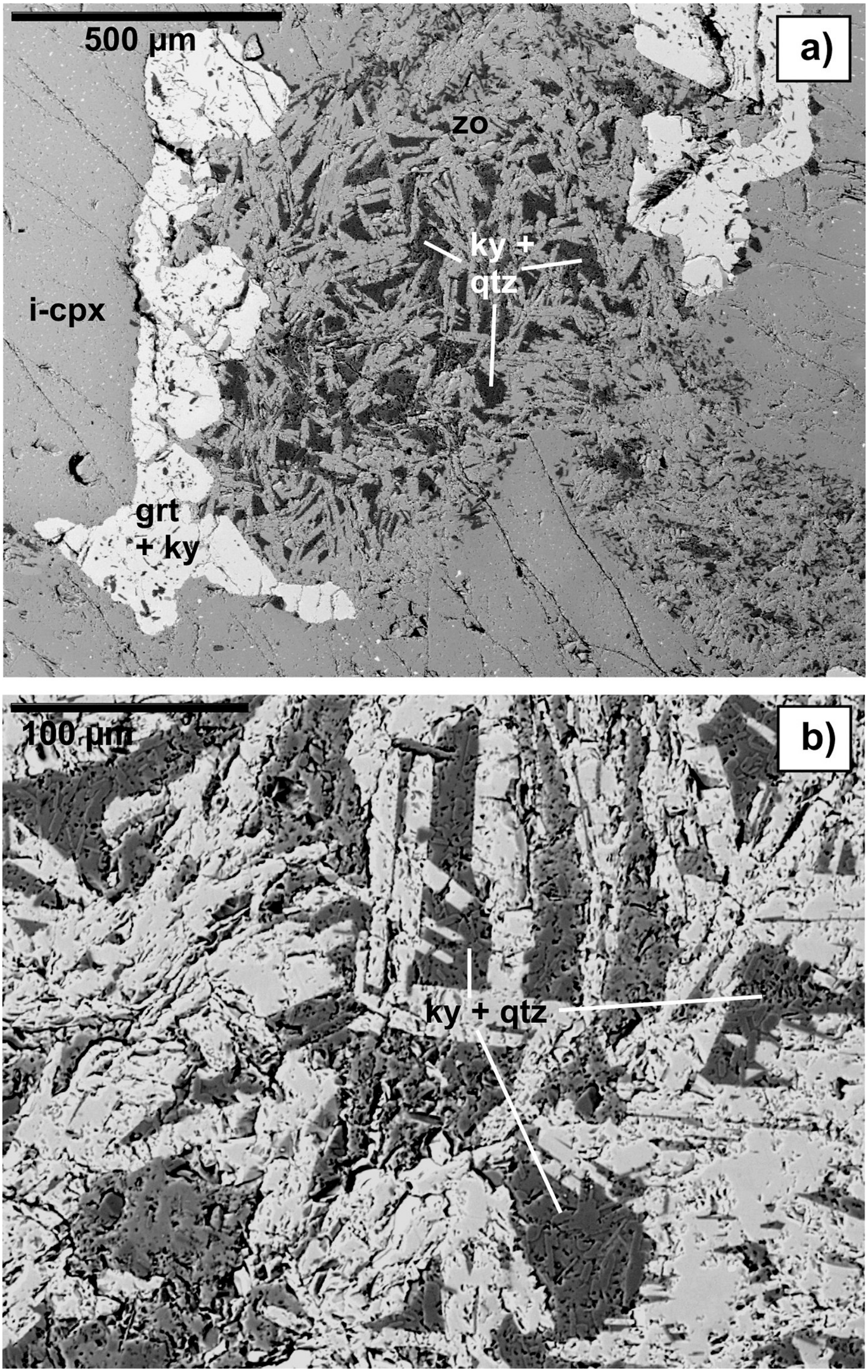

Fig. 6 (4WP): a) strongly coarsened i-plag domain with zoisite and very subordinate m-cpx (both light grey) and kyanite + quartz (dark grey); b) detail of 6a: lath-shaped minerals are zoisite and kyanite respectively;

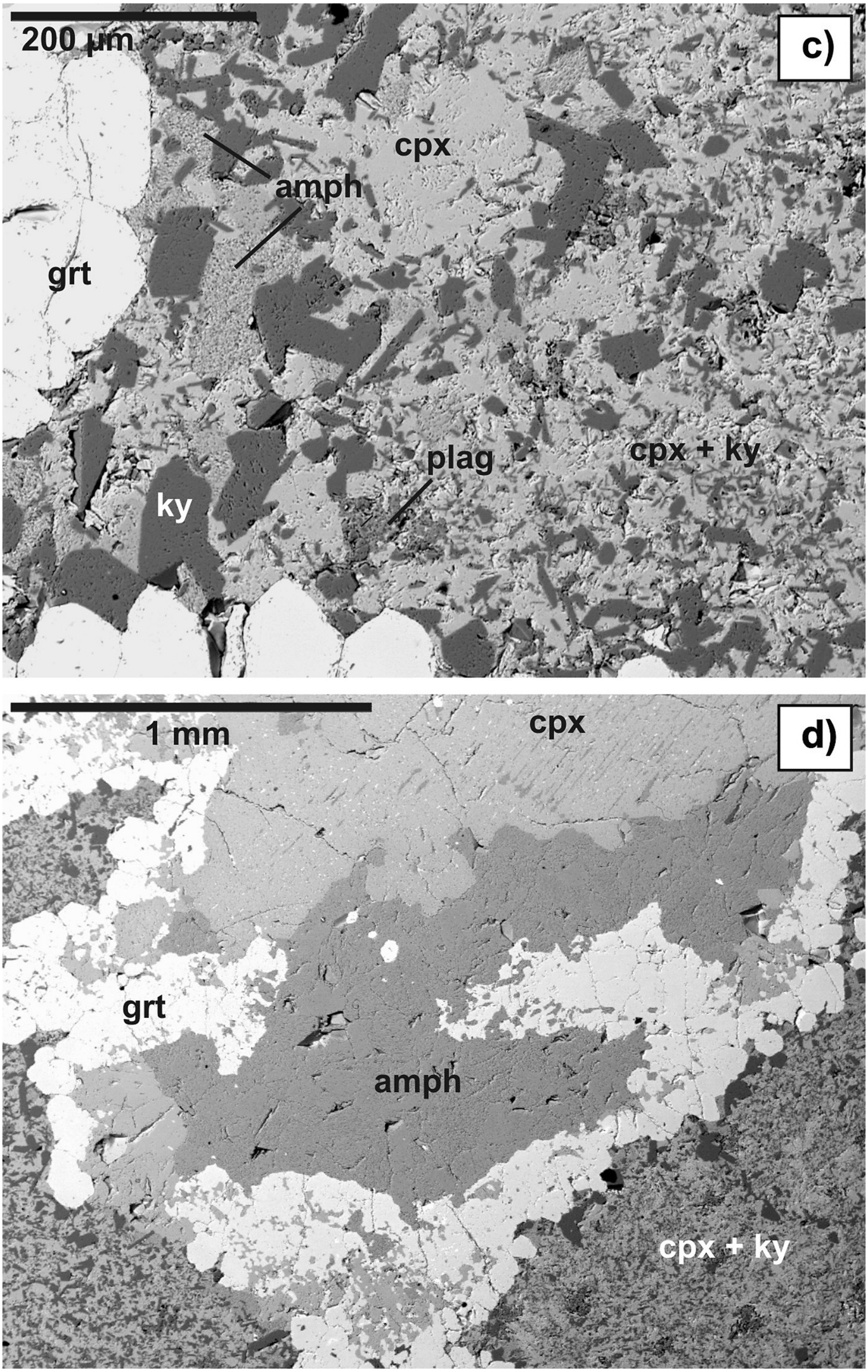

Fig. 6 (4WP): c) coarse grained kyanite and m-cpx near garnet corona; darker grey with bad polish: magnesio-hornblende and (still!) sodic plagioclase; d) magnesio-hornblende enclosed by garnet and m-cpx, adjacent to i-cpx with lamellae of tremolite.

3. Discussion

3.1 Processes and reactions

At this point we will only try a qualitative description of the processes and chemical potential gradients which lead to the evolution of the textures described above. The main reason for that is firstly the uncertainty as to when this short-lived event of transformation has happened during the eo-Alpine high-pressure metamorphic cycle, and hence the uncertainty about *P-T* conditions and absolute values of chemical potentials (µ's) on that basis, because even the most transformed samples at hand show too much disequilibrium for reasonable *P-T* determination with thermodynamic tools. Secondly, this is not a simple problem in 2- or 3-dimensional µ-space, but a multidimensional one, due to the fact that all major cations, Ca, Mg, Al, Si, Na, Fe and H must be considered as variable in space and time throughout the event, as will be shown below. The formal description of reactions must be by open-system reaction equations which can explain the textures observed and which can also consider the relative mobility of ions. The transport medium of these ions was most likely not a true fluid, but a slightly hydrated grain boundary region, characterized mainly by hydrolysis of silicates of the type

$$M^{n+}O_{n/2} + n/2\ H_2O = M^{n+} + n\ OH^-, \qquad (R1)$$

$$\text{for example: } MgO + H_2O = Mg^{2+} + 2\ OH^-, \qquad (R1a)$$

and hence by a front of basicity entering the gabbro. Basicity is reduced to the degree the cation budget can be balanced between different reacting rock domains, for example:

$$Mg_2Si_2O_6 + Ca^{2+} = CaMgSi_2O_6 + Mg^{2+} \qquad (R2)$$

In this simplest form of transformation of opx into cpx, no fluid or basicity front are required, at least for chemical balancing, because charge balance is maintained by cations alone. This would be strictly true for bulk diffusion within or amongst solids. In the presence of additional H_2O, however, not only the transport properties change, but, quite realistically, different diffusion rates for Mg^{2+} and Ca^{2+} would be allowed, because rapidly diffusing OH^- and H_2O would compensate for that. Examples illustrating this more thoroughly will be given below, together with a simple qualitative description of processes and the evolution of the sites of former igneous orthopyroxene (i-opx), clinopyroxene (i-cpx) and plagioclase (i-plag) and their grain boundary regions.

Igneous clinopyroxene is the least reactive of the three major magmatic precursor phases – most likely because it is structurally stable also at eclogite facies conditions and only has to adapt in terms of its solid solution composition to metamorphic clinopyroxene (m-cpx). Igneous plagioclase is characterized by a first, almost isochemical internal decay followed by slow recrystallisation to coarser grain sizes and slow progress of decay assemblage zones towards the core. The compositions of the constituent more or less stable or metastable solid solution phases in this i-plag-domain, metamorphic clinopyroxene (m-cpx) and plagioclase (m-plag), change slightly and somewhat inconsistently throughout the evolution, but the trend is towards more sodic compositions in the core. Magmatic orthopyroxene on the other hand is characterized by corona development and a thickening and change of grain size and type of corona. Quite obviously, both from the macroscopic and microscopic textures, reactions started from the original grain boundaries, triggered by infiltration of minor amounts of molecular hydrous species. The development of a clinopyroxene rim of almost pure diopside composition around orthopyroxene in theory only requires a very simple exchange of Mg for Ca as well as minor structural reconfiguration (R2). The apparent source of Ca was plagioclase, which faced decay into a fine-grained intergrowth of clinopyroxene plus kyanite right at the grain boundary. There must have been a mobilization and loss of Ca at this site, because Ca moves both towards orthopyroxene to form the cpx corona, and towards the plagioclase interior, where decay into albite-rich plagioclase plus zoisite requires addition of both Ca^{2+} and OH^{-}:

$$3\ CaAl_2Si_2O_8 + Ca^{2+} + 2\ OH^{-} = 2\ Ca_2Al_3Si_3O_8(OH) \qquad (R3)$$

The first cpx forming near the original grain boundary has about the same Na/Ca ratio as the original plagioclase (1/3). Balancing a reaction equation with measured mineral compositions and the fastest of the most important mobilized ions (Mg^{2+}, Ca^{2+} and hydrous species), gives:

$$\begin{aligned}&1.00\ \text{i-plag} + 0.42\ Mg^{2+} + 0.28\ OH^{-} =\\ &0.55\ \text{m-cpx} + 0.69\ \text{ky} + 0.17\ \text{m-plag} + 0.28\ Ca^{2+} + 0.14\ H_2O \qquad (R4a)\end{aligned}$$

In order to compare with observed mineral modes, one can assign first-order volume by multiplying with the number of oxygens in each mineral or species (no volume for metal ions):

$$\begin{aligned}&8.00\ \text{i-plag} + Mg^{2+} + 0.28\ OH^{-} =\\ &3.31\ \text{m-cpx} + 3.45\ \text{ky} + 1.38\ \text{m-plag} + Ca^{2+} + 0.14\ H_2O \qquad (R4b)\end{aligned}$$

Under these conditions of formal, first-order balance of charge and volume, the approximately equal modes of m-cpx and kyanite observed in thin section are reproduced; only the amount of m-plag could be slightly over-estimated.

However, the original grain boundaries between i-plag grains are in some places outlined by corundum and, even more importantly, the original grain boundaries between i-plag and i-opx are marked by a corona, which, in its first evolutionary stage, shows myrmekitic intergrowth of new metamorphic clinopyroxene with subordinate spinel and, in places, corundum. A simple replacement of orthopyroxene by clinopyroxene according to reaction (R2) would not release any Al because the amount of Al and Si contained in both minerals is almost identical (Tab. 1) during this first stage of corona formation. Al must be derived from the plagioclase site, which can be tested by modifying (R4) in order to see, if Al can be released. In this case, O-H-species cannot be included in this simple type of reaction equation:

$$\begin{aligned}&1.00\ \text{i-plag} + 0.46\ Mg^{2+} =\\ &0.62\ \text{m-cpx} + 0.62\ \text{ky} + 0.14\ \text{m-plag} + 0.23\ Ca^{2+} + 0.16\ Al^{3+} \qquad (R5a)\end{aligned}$$

or in terms of volume:

$$\begin{aligned}&8.00\ \text{i-plag} + Mg^{2+} =\\ &3.73\ \text{m-cpx} + 3.11\ \text{ky} + 1.17\ \text{m-plag} + Ca^{2+} + Al^{3+} \qquad (R5b)\end{aligned}$$

Equations 4 and 5 in combination with the observed textures suggest that both Ca^{2+} and Al^{3+} are being mobilized at the plagioclase site and transported into and through the corona, in exchange for Mg^{2+}. Hydrous species must have been involved additionally, so the overall reaction is a complex combination of reactions 4, 5 and others of minor importance. The surprising mobility of Al^{3+} may in fact be due to the high pH of the hydrous transport medium. It comes as no surprise that mobilized Al^{3+} would now react with Mg^{2+} and Fe^{2+} expelled from the opx-site to form spinel, but it is less clear, why it should precipitate as corundum within, and later preferentially on both sides of the corona, nor is it clear, why it should outline former boundaries between plagioclase grains. At each of these sites, the solubility of Al^{3+} must have dropped, either because the pH changed in a more open (fluid-like) pore space or because other ions precipitated, like Ca^{2+} forming cpx at the opx grain boundary, but at this point in time, these can be only speculations.

The garnetization of the corona and the replacement of corundum by kyanite on the other hand can be easily explained by the increase of the chemical potential of SiO_2 due to a continuing transformation of the albite component of relict plagioclase into jadeite and SiO_2 which results in an increase in jadeite component in clinopyroxene at its various growth sites and in transport of SiO_2 down its chemical potential gradient, i.e. mainly into and across the coronas around relict opx, until the chemical potential is finally high enough for quartz to become stable. The first formation of corona garnet is by:

diopside (in cpx) + spinel + SiO_2 = garnet (R6),

thus causing both consumption of spinel and a modal decrease in corona clinopyroxene. Interestingly, garnet does not form by the simple reaction

orthopyroxene + corundum + Ca^{2+} = garnet + Mg^{2+} (R7)

because corundum is preferentially replaced by kyanite. Reaction (R 7) however may become relevant at a late stage for corundum at the opx-boundary of the corona (Fig. 6d). Hence, after exhaustion of spinel, garnet further grows from clinopyroxene + kyanite according to:

0.9 cpx + 1 ky + $1.2\ Mg^{2+} + 0.2\ Si^{4+} + 3.2\ OH^{-}$ = 1 grt + $1.6\ H_2O$ (R8a)

This reaction is valid for garnet growth (and cpx-replacement) inside the corona as well as for garnet overgrowing the clinopyroxene-kyanite intergrowths of the plagioclase site.

At some stage during continuing hydration the fugacity of H_2O has become high enough inside the corona to trigger transformation of remaining orthopyroxene into an amphibole of at first tremolite and later of more Na- and Al-rich magnesio-hornblende composition. These compositions illustrate that all elements are mobile, not just the ones used in the simplified equations above, but we hope to have nevertheless found a way to describe the most important transport processes and mineral reactions in a field of chemical potential gradients which drop for Mg^{2+} and Fe^{2+} from orthopyroxene outwards and for Ca^{2+}, Na^{2+}, Al^{3+} and Si^{4+} from the plagioclase site outwards, with a short temporal delay for Na^{2+}, and Si^{4+} in the latter case because of metastable perseverance of sodic plagioclase. A higher H_2O fugacity is also recorded in the inner parts of metastable igneous clinopyroxene, where tremolite forms along cpx cleavage planes. The smoothing out of composition gradients in garnet and clinopyroxene across the coronas and between different textural sites indicates the relaxation of initially steep chemical potential gradients and an increase in volume of *effective bulk composition*. We attribute this phenomenon mainly to the length of time during which hydrous species were available to facilitate reactions – a time span that was definitely short-lived, as otherwise the entire texture would have been obliterated.

3.2 Comparison with other eclogitized metagabbros worldwide

There are a considerable number of reports in the literature about coronitic metagabbros that have experienced a sudden and short-lived metamorphic reactivation and transformation at conditions near or inside the eclogite facies. The main observations can be summarized as follows: In most examples olivine was present in addition to plagioclase, ortho- and clinopyroxene or instead of orthopyroxene. In virtually all cases olivine developed an inner corona of orthopyroxene as well as an outer corona of diopsidic (to sometimes slightly omphacitic) composition (Mørk 1986; Wayte & al. 1989; Gilotti & Elvefold 1998; Cox & Indares 1999; Lang & Gilotti 2001). In more strongly overprinted samples, olivine can be completely replaced by orthopyroxene (e.g. Cox & Indares, 1999), but also by amphiboles, omphacite and talc (Pognante 1985; Mørk 1985; Engvik & al. 2001). The boundary towards the plagioclase domain is quite consistently marked by a garnet corona, but here the differences set in as various other minerals can be included, mostly clinopyroxene, zoisite and kyanite, but also mafic phases (Wayte & al. 1989; Engvik & al. 2001). Thickening and chemical homogenization of the corona garnet is again a rather general feature of progressive overprinting.

Less attention is usually given to magmatic orthopyroxene, as the textural evolution around olivine seems to be the more spectacular one. There is only one report about symplectitic clinopyroxene-spinel intergrowths replacing orthopyroxene (which forms an outer corona around olivine), by Whitney & McLelland (1973), but their clinopyroxenes are very poor in sodium and the corona growth was supposed to have taken place in the granulite rather than in the eclogite facies.

The evolution of magmatic clinopyroxene is described very consistently as unspectacular: development of more jadeitic growth rims and slow internal recrystallization with a compositional trend towards omphacite and replacement of ilmenite inclusions by rutile.

The most variable textural setting is that of igneous plagioclase. Even in the simplest case of a virtually bimineralic clinopyroxene-plagioclase gabbro, Miller (1970) describes the plagioclase as "saussuritized", i.e. decomposed into a light-coloured, fine-grained aggregate of phases, which could be identified by X-ray diffraction as kyanite + plagioclase + zoisite ± quartz ± clinopyroxene. Wayte & al. (1989) performed a detailed transition electron microscopic (TEM) study on the inner plagioclase domain remote from any corona, and distinguished three zones with different degree of replacement: The innermost zone with <10 % replacement looks like unaltered plagioclase under the light microscope, but TEM-imaging reveals sub-micron scale clinozoisite of 0.1–0.4 µm diameter. An adjacent zone with 10–50 % transformation contains larger (2–4 µm) grains of zoisite, kyanite, quartz and Na-enriched plagioclase, and in the outermost zone of this inner domain more than 50 % of the original plagioclase has transformed into jadeite + kyanite + zoisite + quartz. The grain size is sub-micron again, and new plagioclase is the most Na-rich, but can only be detected by TEM. The more advanced stage of replacement of primary plagioclase as preserved in a metagabbroic rock from the Western Gneiss Region in Norway (Engvik & al. 2001) is characterized by fine-grained clinozoisite, kyanite, omphacite, quartz, paragonite and garnet.

In the majority of cases, however, highly Al-rich phases have been observed at the plagioclase site, quite in contrasts to the Gressenberg samples: The igneous plagioclase of an olivine-metagabbro from Flemsøy, Western Norway (Mørk 1985, 1986) is replaced initially by metamorphic sodic plagioclase and acicular spinel, and at a more advanced stage by garnet and omphacite. In a gabbro-norite from Northeast Greenland (Gilotti & Elvefold 1998) the plagioclase site is characterized by needles of kyanite and zoisite, and in one case contains some corundum. These phases are later overgrown by garnet and omphacite. Cox & Indares (1999) report that plagioclase relicts contain abundant spinel and, locally, corundum. Finally, Lang & Gilotti (2001) describe eclogitized olivine-bearing gabbros from Greenland in which one type of replacement texture of former plagioclase represents an early stage: it has relict plagioclase in the core, surrounded by an omphacite-spinel symplectite, with some corundum and amphibole at the outer margin, and a layer/corona of omphacite towards orthopyroxene.

In the light of our own observations on the Gressenberg samples, we can only attempt a very broad and general summary interpretation of these findings from other eclogitized coronitic metagabbros, and particularly of the processes and chemical potential gradients leading to such varied evolution of the plagioclase site. As boundary conditions, we have the original magmatic textural settings and compositions of mineral grains, the degree of deviation from thermodynamic equilibrium (the "delta G" of reactions) and relative diffusion rates and pathways of hydrous species and, as the case may be, dissolved and transported ions. If the degree of overstepping is high compared to the transport capacity of the incoming "fluid", a relatively instant local decay of plagioclase to a (more) stable mineral assemblage happens, with very small volumes of equilibration.

This process could be considered isochemical. Examples would be the textures described by Wayte & al. (1989). If, or as soon as, transport capacity is more equivalent to reaction capacity, earlier textures would tend towards equilibration on a larger scale and other reactions would become possible, such as those described in this paper. The main chemical potential gradients as described earlier – those for Mg and Fe are decreasing away from olivine and to a lesser degree from orthopyroxene, and those of Ca and Na, as well as Al and Si decreasing away from the plagioclase site – are responsible for the evolution of textures.

But given such generality, what explains the differences? We can offer one general answer for the textural positioning of Al-rich phases. Only in those cases, when there was no olivine in the precursor rock (Whitney & McLelland 1973; Kunze & al. 2007; this work) would Al be transported towards the decomposing orthopyroxene and become part of the evolving corona. In most other cases the more extreme release (higher chemical potential) of Mg^{2+} and Fe^{2+} from olivine towards the environment does not allow much ion exchange towards olivine other than Ca and traces of Na and Al to form an outer corona of clinopyroxene and later garnet. The Al of decomposing anorthite component remains in the plagioclase site and reacts with incoming Mg and Fe to spinel, e.g. in the form of a clinopyroxene-spinel symplectite (Lang & Gilotti 2001) and further away from the incoming ion front to corundum, kyanite and zoisite, and is responsible for the formation of garnet at the plagioclase site at a later stage (e.g. Lang & Gilotti 2001)

It should be noted that the work of Wayte & al. (1989) is the only one of those described above, which employed a high-resolution instrument to these problematic fine-grained textures. In most other cases not even electron microscope images were used for documentation but only thin section photomicrographs. Any reactions given were formulated in mineral endmembers, sometimes including ions, but never balanced for charge or even oxygens.

Hence, there is still ample space for improvement to understand the broader picture told by the quite varied textures and compositions observed at different localities, but occasionally even within one sample suite or thin section. A more detailed investigation including geothermobarometry (determination of pressure and temperature) on the most equilibrated parts of samples and quantitative chemical potential phase diagrams should point the way.

Acknowledgements

Mr. Franz Fürntratt (formerly at Universalmuseum Joanneum) is thanked for the preparation of the thin sections. The generous donation of blocks by the land owner, Mr. Markus Freydl from Gressenberg and the generous and careful editorial handling of K. Stüwe have been instrumental for this paper to see the light of day. May it be an inspiration for others to seek the answers to nature's enigmatic beauties both on the large and on the very small scale.

References

Bruand E., Stüwe K. & Proyer A. 2010: Pseudosection modelling for a selected eclogite body from the Koralpe (Hohl), Eastern Alps. – Mineralogy and Petrology 99: 75–87.

Engvik A. K., Austrheim H. & Erambert M. 2001: Interaction between fluid flow, fracturing and mineral growth during eclogitization, an example from the Sunnfjord area, Western Gneiss Region, Norway. – Lithos 57: 111–141.

Gilotti J. A. & Elvefold S. 1998: Partial eclogitization of the Ambolten gabbro-norite, North-eastern Greenland Caledonides. – Schweizerische Mineralogische und Petrographische Mitteilungen 78: 273–292.

Gregurek D., Abart R. & Hoinkes G. 1997: Contrasting Eoalpine P-T evolutions in the southern Koralpe, Eastern Alps. – Mineralogy and Petrology 60: 61–80.

Heritsch H. 1973: Die Bildungsbedingungen von alpinotypem Eklogitamphibolit und Metagabbro, erläutert an Gesteinen der Koralpe, Steiermark. – Tschermaks Mineralogische und Petrographische Mitteilungen 19: 213–271.

Kunze R., Tropper P. & Konzett J. 2007: Petrologische und experimentelle Untersuchungen zum Gabbro-Eklogitübergang am Bärofen (Steiermark) . – Mitteilungen der Österreichischen Mineralogischen Gesellschaft 153: 72.

Lang H. M. & Gilotti J. A. 2001: Plagioclase replacement textures in partially eclogitised gabbros from the Sanddal mafic-ultramafic complex, Greenland Caledonides. – Journal of metamorphic Geology 19: 497–517.

Miller Ch. 1970: Petrology of some eclogites and metagabbros of the Oetztal Alps, Tirol, Austria. – Contributions to Mineralogy and Petrology 28: 42–56.

Mørk M.-B. 1985: A gabbro to eclogite transition on Flemsøy, Sunnmøre, Western Norway. – Chemical Geology 50: 283–310.

Mørk, M.-B. 1986: Coronite and eclogite formation in olivine gabbro (Western Norway): reaction paths and garnet zoning. – Mineralogical Magazine 50: 417–426.

Pognante U. 1985: Coronitic reactions and ductile shear zones in eclogitised ophiolite metagabbro, Western Alps, North Italy. – Chemical Geology, 50, 99–109.

Postl W. 2009: Geopark Glashütten – Ein Führer durch die Gesteinswelt der Koralpe. – 89 Seiten, Verlag Geologische Bundesanstalt, ISBN: 978-3-85316-051-0.

Thöni M. & Jagoutz E. 1993: Isotopic constraints for Eo-Alpine high-P metamorphism in the Austroalpine nappes of the Eastern Alps: bearing on Alpine orogenesis. – Schweizerische Mineralogische und Petrographische Mitteilungen 73:177–189.

Thöni M. & Miller C. 1996: Garnet Sm-Nd data from the Saualpe and Koralpe (Eastern Alps, Austria): chronological and PT constraints on the thermal and tectonic history. – Journal of metamorphic Geology 14: 453–466.

Weber A. 1941: Gabbro und Gabbroabkömmlinge von der Koralpe (Steiermark). – Zentralblatt für Mineralogie, Geologie und Paläontologie, Abt. A, Jg. 1941, 209–216.

Whitney P. R. & McLelland J. M. 1973: Origin of coronas in metagabbros of the Adirondack Mts., N. Y. – Contributions to Mineralogy and Petrology 39, 81–98.

Winkler A. 1966: Die Verbreitung der eklogitischen Gesteine von Gressenberg bei Schwanberg, Weststeiermark. – Mitteilungen des naturwissenschaftlichen Vereines für Steiermark 96: 112–120.

Mitteilungen des naturwissenschaftlichen Vereines für Steiermark | Bd. 140 | S. 68 | Graz 2010

Buchbesprechung / Book Review

Variation – ein Jahr faszinierende Naturfotografie aus NaturFoto. 2009. – 128 Seiten, 135 Abbildungen. Tecklenborg-Verlag, Steinfurt. Querformat 26,5×24 cm. ISBN 978-3-939172-44-4. Preis € 24,50. Werk ohne Angabe von Autoren.

Diese Neuerscheinung – mehrere Dutzend Fotografen sind daran beteiligt – stellt ein Sammelwerk der besten Bilder aus dem Vorjahr dar. Es ist ein sehenswerter Bilderbogen, der dem Beschauer präsentiert wird. Er spannt sich von grandiosen, teils stimmungsvollen Landschaftsaufnahmen, über eindrucksvolle Wildtierfotos, bis hin zu faszinierenden Bildern aus dem Bereich der Makrofotografie. Eine Auflistung der Kapitel zeigt die Vielzahl der im Detail angeschnittenen Themen: Bergwelten, Bären, Vögel, Grün, Gorillas, Blumen, Frost, Nebel, Reptilien & Amphibien, Wälder, Fuchs & Wolf, Stimmungen, Afrika, Landschaften, Insekten.

Die gezeigten Fotos haben durchwegs eine so starke Ausdruckskraft, dass es genügt, die Legenden nur kurz zu halten. Leider treten auf den Seiten 77, 120/21 sowie 123 ein paar Unkorrektheiten auf, die sich leicht hätten vermeiden lassen. Die Faszination des gebotenen Bildmaterials ist davon allerdings in keiner Weise betroffen.

Durch den Bilderreichtum und den moderaten Preis ist dieser Band geradezu prädestiniert, als wertvolles Buchgeschenk für Naturliebhaber und an der Naturfotografie interessierte Personen verwendet zu werden.

Reinhart Schuster